

Paleomagnetically derived folding rates, southern Pyrenees, Spain

James E. Holl } Department of Earth and Environmental Sciences, Lehigh University, Bethlehem,
David J. Anastasio } Pennsylvania, 18015-3188

ABSTRACT

Well-dated syntectonic unconformities with the Spanish Pyrenees allow characterization of sedimentation and deformation within an orogenic foreland. The Spanish Pyrenees are composed of a south-vergent thrust belt and foreland basin in which folds developed both parallel and perpendicular to tectonic transport. Unconformity geometries and magnetostratigraphic data from synorogenic strata provide a precise temporal framework for the quantitative analysis of the Mediano anticline, the largest of the transverse folds. Folding began in the early Eocene and ended by ~42 Ma at which time an anticline 20 km long and ~5 km in wavelength had been produced. Angular and progressive unconformities within syntectonic sedimentary units preserve the history of fold development. Fold growth resulted from westward salt movement driven by prograding sediments and was characterized by 2–3 m.y. intervals of slow continuous limb tilting, 2.2°–4.2°/m.y., preserved as progressive unconformities within syntectonic strata. Because the emplacement of the Cotiella-Montsec thrust sheet was episodic, intervals of slow fold growth were punctuated by intervals lasting <1.5 m.y. when fold growth was three to ten times faster, producing angular unconformities.

INTRODUCTION

Synorogenic strata provide a record of tectonic activity within a mountain belt, but incomplete exposures and lack of accurate chronologic markers often make direct links between sedimentation and deformation difficult. Within the Spanish Pyrenees, some folds developed in an actively aggrading foreland basin where unconformity geometries allow direct links between deformation and deposition. By establishing a precise chronology for these synorogenic strata, it is possible to determine sedimentation and deformation rates and characterize the transient nature of fold growth within mountain belts.

Traditionally, unconformities are thought to represent erosion, however, unconformities may also result from continuous aggradation during orogenesis. Synorogenic unconformities can be classified as progressive unconformities, which result from slow tilting of the depositional surface with respect to sedimentation rate, or angular unconformities, which result from rapid tilting of the depositional surface with respect to sedimentation rate (Riba, 1976). In the south Pyrenean foreland, both types of unconformities were observed within the synorogenic deposits around the Mediano anticline, a regional-scale transverse fold (Fig. 1). Magnetostratigraphic data provide a temporal framework, which is used to reconstruct the deformational and depositional history of the Mediano area. The reconstructions permit a quantitative assessment of the relation between unconformity geometries and the rates of deformation and sedimentation. Thrust emplacement, fold development, and sedimentation are transient orogenic proc-

esses. Synorogenic strata around the Mediano anticline preserve a detailed record of fold growth, permitting a rare glimpse of temporal variations in progressive deformation rates and an assessment of driving forces for Pyrenean folding.

GEOLOGIC SETTING

Pyrenean orogenesis produced thrust belts and foreland basins within both the Iberian and European plates. A series of synsedimentary folds oriented both parallel and perpendicular to tectonic transport developed within the Spanish foreland (Anastasio, 1992), which became detached during continued orogenesis (Ori and Friend, 1984; Labaume et al., 1985). The origin of many transport-parallel structures has been attributed to several mechanisms, including prethrust buckling (Séguret, 1972), movement over an

oblique ramp (Dérmond et al., 1984), and salt deformation (Anastasio, 1992).

The Mediano anticline is a transverse décollement fold with a wavelength of ~5 km and a strike length of ~20 km and is cored by >2 km of Triassic evaporites, which in part are concordant with and in part diapiric with respect to overlying strata (Fig. 1). Upper Eocene carbonate rocks on the crest and flanking deeper water shales led Puigdefábregas (1974) to postulate early Eocene fold initiation. Subsequent fold growth is recorded by angular and progressive unconformities within Eocene strata flanking the anticline. Syntectonic sedimentation around the anticline included siliciclastic turbidites and mudstones derived from exposures of the Gavarnie and Cotiella-Montsec thrust sheets to the north, south, and east, which were deposited in 400–1000 m of water (Fig. 1; Mutti et al., 1989). Folding-induced submarine topography channelled paleocurrents northward along the slope until the late middle Eocene. Infilling of the foreland basin by westward progradation of coastal deposits is recorded around the Mediano anticline as a transition from slope turbidites and mudstones to shelf and nearshore detrital rocks up section.

PALEOMAGNETIC STUDY

To determine deformation and sedimentation rates, magnetostratigraphic data were obtained from synorogenic strata surrounding the Mediano anticline. Between two and four samples, spaced over ~2 m of section,

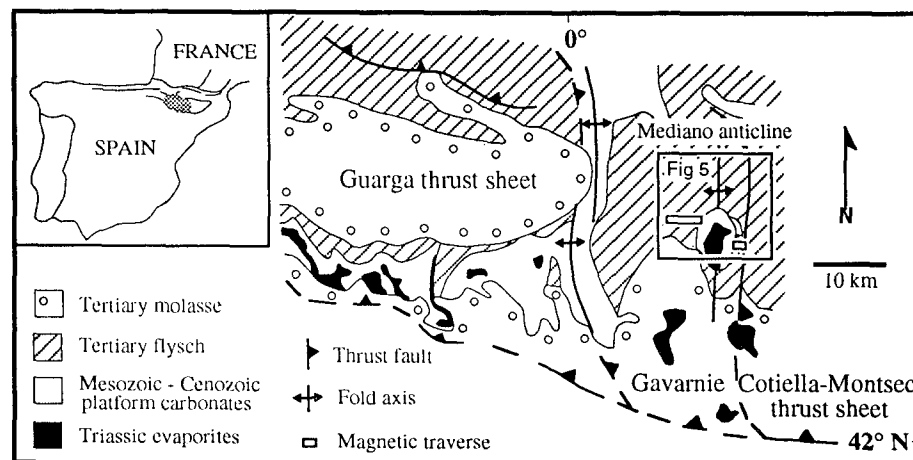
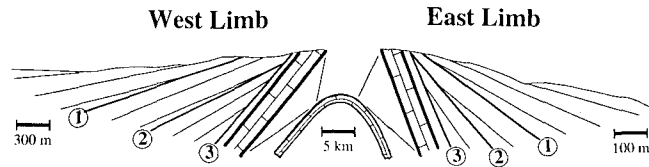


Figure 1. Generalized geologic map of Spanish Pyrenees.

Figure 2. Unconformity geometries flanking Mediano anticline. Angular unconformities numbered here and on subsequent figures.



were collected at sites located at stratigraphic intervals of ~40 m along traverses through both limbs of the fold (Figs. 1, 2). The recurrence interval of polarity reversals in the Eocene permits the history of deformation and sedimentation to be determined with a resolution of ~0.5 m.y.

Samples from each rock type were demagnetized with thermal and alternating-field methods to determine the optimal demagnetization strategy for the remaining samples. Thermal demagnetization was more effective in cleaning the very weakly magnetized (10^{-1} – 10^{-2} mA/M) samples. Above 400 °C, magnetic intensity increased rapidly, and magnetic vectors became inconsistent as iron sulfides were transformed to magnetite during heating (Fig. 3; Burbank et al., 1992). During thermal demagnetization between 250 and 400 °C, the magnetization of most samples maintained nearly constant directions as the intensity decreased, which is consistent with isolation of the characteristic magnetization (Fig. 3). On the basis of the results of the pilot study, the remaining samples were demagnetized in 25° steps between 250 and 400 °C. The characteristic magnetization for each sample was determined by principal-component analysis (Kirschvink, 1980). To ensure accuracy, only samples (80% of total) with a maximum angular deviation <15° were used to determine horizon polarities. A fold test of the calculated di-

rections suggests that the characteristic magnetization was recorded during folding, a result consistent with isolation of the primary depositional magnetization.

The polarity of each sampling horizon was assigned, using the criteria of Hillhouse et al. (1977), on the basis of the characteristic remanence. To eliminate the effects of secular variation, a horizon was considered reversed if at least one of the samples fell within 30° of the Eocene reversed axial dipole [$I = -63^\circ$, $D = 180^\circ$]. A horizon was considered normal if no sample was reversed and at least one sample had a characteristic direction that fell within 30° of the Eocene normal axial dipole [$I = 63^\circ$, $D = 0^\circ$] (Roest and Srivastava, 1991). A horizon was considered indeterminate (1 of 36) if none of the measured directions was within 30° of either the normal or reversed dipole after demagnetization. Horizon polarities were used to establish magnetostratigraphic sections for both limbs of the Mediano anticline, with most reversals confirmed by multiple sampling horizons (Fig. 4).

The sampled stratigraphic sections consist of the Castisent Group, the Santa Liestra Group, and the lower Campodarbe Group (Mutti et al., 1989). Biostratigraphic data used to correlate the magnetostratigraphic data to the geomagnetic polarity time scale include (1) the nannoplankton *Discoaster lodoensis* (Marzo et al., 1988) of nannoplank-

ton zone 13 (52–50.5 Ma) in the Castisent Group, (2) fauna from mammal level MP 13 (47–48 Ma) found in shelf deposits correlative to the Santa Liestra Group, (3) fossils of MP 14 (46–45 Ma) from the upper Santa Liestra equivalent (Gozalo, 1989), and (4) fossils from mammal level MP 15 (41–42 Ma) within the lower-middle Campodarbe group (Gozalo, 1989). The coincidence of the observed unconformity geometries and similarity of the magnetic polarity records for both limbs provides confidence that the magnetostratigraphic correlation is accurate (Figs. 2, 4).

DISCUSSION

Geologic and geochronologic data permit us to reconstruct the history of fold development and sedimentation at >51, 48, 46, and 42 Ma (Fig. 5). Rocks deposited on the flanks of the Mediano anticline were backstripped and corrected for compaction in the reconstructions (Sclater and Christie, 1980). Time-averaged sedimentation rates calculated for each polarity chron averaged 200 m/m.y. ($\sigma = 60$ m/m.y.) for the west limb and 70 m/m.y. ($\sigma = 30$ m/m.y.) for the east limb. Ages of angular unconformities were estimated by interpolation between polarity chron boundaries using measured rates of sediment accumulation. These ages provided a temporal framework in which to reconstruct the tilted angular and progressive unconformities and to calculate the rates of limb tilt, uplift, and shortening for the Mediano anticline.

Differences in sedimentation rates within the sections were used to calculate the maximum possible depositional hiatus represented by the angular unconformities. A favored estimate of folding rate (limb tilt), ~20°–40°/m.y., was calculated for each angular unconformity using hiatus duration (Fig. 6). A minimum folding rate of 10°–13°/m.y. was calculated by assuming that the time missing at the unconformity was no greater than the duration of the polarity chron containing it. Given the aggradational history of the basin and the consistency of time-averaged sedimentation rates, large depositional hiatuses are clearly unreasonable. The intervals of more rapid limb tilting represented by angular unconformities punctuate, at 2–3 m.y. intervals, the intervals of slow continuous tilting recorded as progressive unconformities. Rates of limb tilt calculated for intervals represented by progressive unconformities ranged from 2.2° to 4.2°/m.y. for both limbs, about three to ten times slower than the rates recorded by the angular unconformities (Fig. 6).

Temporal variations in folding rates relate to tectonic processes active within the evolving south Pyrenean foreland. An uplift rate of

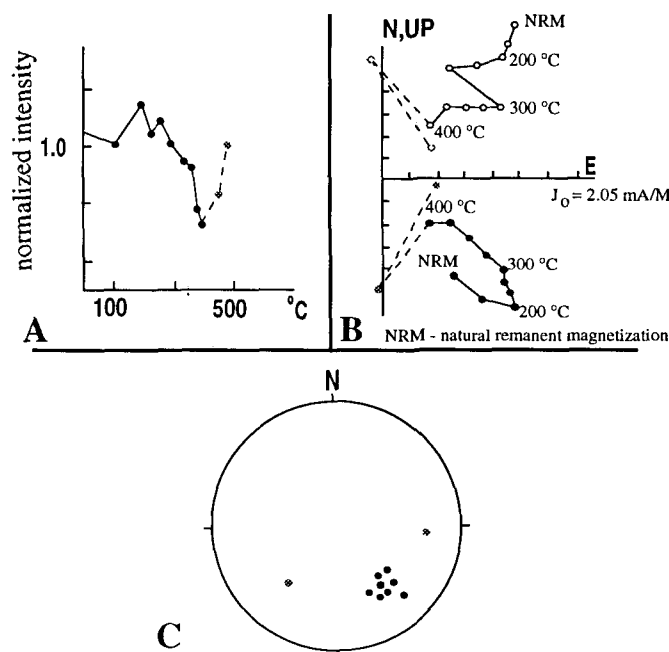


Figure 3. Characteristic demagnetization behavior of representative sample. A: Normalized intensity. B: Orthogonal endpoint projection; open symbols represent vertical (closed symbols represent south) vs. east component of magnetization, J_0 = initial magnetization (Zijderveld, 1967). C: Stereographic plot of magnetic direction at each step.

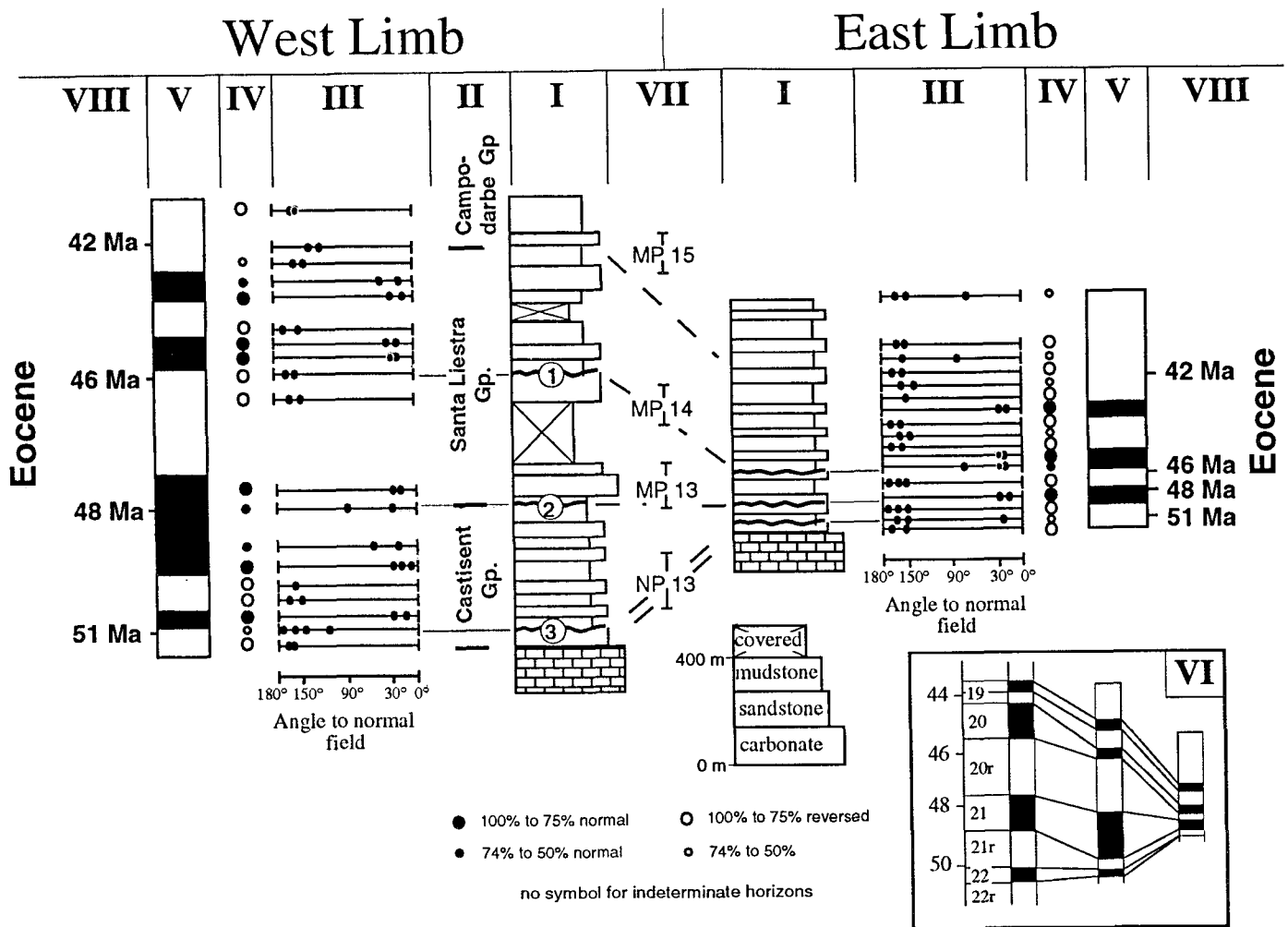


Figure 4. Mediano anticline magnetostratigraphies. I: Thickness and lithology of sampled sections. II: Stratigraphic nomenclature. III: Position of sampling horizons and characteristic remanent magnetic direction of individual, progressively demagnetized samples. IV: Horizon polarity summaries for each limb. V: Magnetic reversal stratigraphy. VI: Biostratigraphic tie points. VII: Geomagnetic reversal time scale (Harland et al., 1990). VIII: Geochronology.

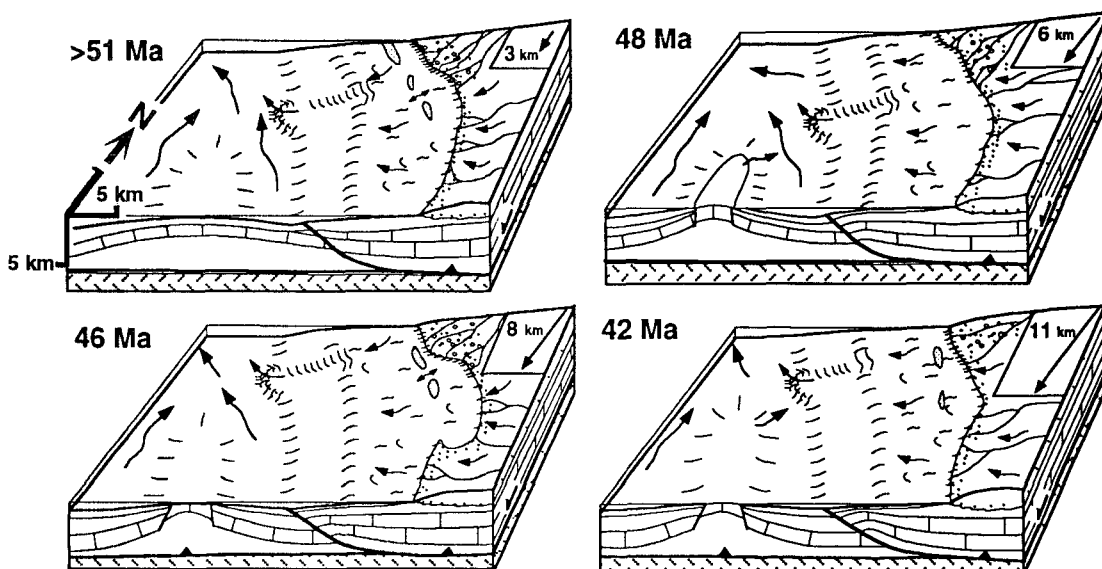


Figure 5. Reconstructed history of Mediano anticline region (paleogeography after Nijman and Nio, 1975). Insets show transport direction and cumulative displacement on Cotiella-Montsec thrust.

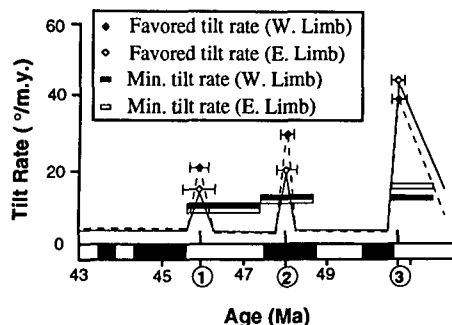


Figure 6. Graph of favored and minimum deformation rates for Mediano anticline. Geomagnetic reversal time scale is shown on horizontal axis with identification numbers (circled) of angular unconformities.

~250 m/m.y. and a horizontal shortening rate of ~500 m/m.y. were calculated from the regional paleogeographic and structural reconstructions (Fig. 5). The average rate of the westward advance of continental facies resulting from both fault movement and sediment progradation was ~500 m/m.y. (Fig. 7). The rate of progradation can be partitioned into a time-averaged rate of ~200 m/m.y. for the westward component of thrust motion and ~300 m/m.y. for sediment progradation (Fig. 7). These values remained nearly constant throughout fold development. Synchronous with westward facies progradation, the entire foreland was translated southward at a rate of ~900 m/m.y.

The similarity between average rates of westward facies progradation and rates of fold growth adds further evidence that these two processes are linked. Differential loading halotectonics (salt flowage resulting from tectonics) has been recognized as an important folding mechanism in the Gulf Coast (Jackson and Talbot, 1986), the Spanish Pyrenees (Anastasio, 1992), and elsewhere. Intervals of rapid fold growth may have resulted from episodic movement of the Cotiella-Montsec thrust sheet. Episodic fold growth is consistent with decollement folding driven by movement of the Cotiella-Montsec thrust sheet (Stein, 1983). The growth of the Mediano anticline and by inference other transverse folds within the south Pyrenean foreland progressed slowly and continuously as a result of salt movement driven by sedimentary loading, and more rapidly as a result of episodic thrust loading.

CONCLUSIONS

The Mediano anticline is a regional-scale structure that developed synchronously with sedimentation, thrusting, and halotectonics within the south Pyrenean foreland. Magnetostratigraphic data provide a temporal framework for analyses of folding and sedimentation and permit a detailed history of fold growth to be reconstructed. Folding be-

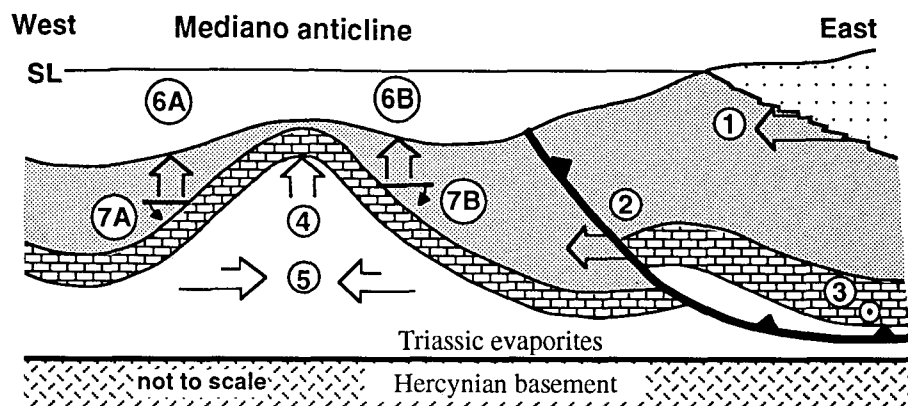


Figure 7. Schematic section summarizing average rates (~51–43 Ma) of (1) westward continental facies progradation (500 m/m.y.), (2) westward component of thrust sheet motion (200 m/m.y.), (3) southward component of thrust-sheet motion (900 m/m.y.), (4) crestal uplift (250 m/m.y.), (5) horizontal shortening (500 m/m.y.), (6) sedimentation rates for both limbs (A—200 m/m.y.; B—70 m/m.y.), and (7) limb tilt for both limbs (A—6.5°/m.y.; B—7.5°/m.y.).

gan in the early Eocene, lasted ~10 m.y., and was characterized by intervals of slow and constant fold growth (2.2°–4.2°/m.y.) punctuated by episodes of deformation three to ten times faster. The slow intervals of limb tilt are recorded by progressive unconformities within syntectonic strata and are likely produced by sediment loading, whereas the intervals of rapid fold development resulted in a series of angular unconformities that can be related to episodic movement of the Cotiella-Montsec thrust sheet.

ACKNOWLEDGMENTS

Funded by National Science Foundation grant EAR-8816335 awarded to Anastasio and by grants to Holl from the American Association of Petroleum Geologists, Sigma Xi, and the Geological Society of America. We thank C. Hedlund for field assistance; K. Kodama for advice and the use of his paleomagnetic laboratory; and S. Boyer, J. Geissman, R. Gordon, P. Heller, J. Hillhouse, and J. Munoz for constructive reviews of the manuscript.

REFERENCES CITED

- Anastasio, D.J., 1992, Structural evolution of the External Sierra, southern Pyrenees, Spain, in Mitra, G., and Fisher, G.W., eds., *Structural geology of fold and thrust belts*: Baltimore, Maryland, Johns Hopkins University Press, p. 239–251.
- Burbank, D.W., Verges, J., Munoz, J.A., and Bentham, P., 1992, Coeval hindward- and forward-imbicating thrusting in the central southern Pyrenees, Spain: Timing and rates of shortening and deposition: *Geological Society of America Bulletin*, v. 104, p. 3–17.
- Déramond, J., Fischer, M., Hossack, J., Labaume, P., Séguret, M., Soula, J.C., Viillard, P., and Williams, G., 1984, Field guide of conference trip to the Pyrenees (Chevauchement et Déformation Conférence): Toulouse, France, Paul Sabatier University, 28 p.
- Gozalo, M.C., 1989, Sedimentary facies and sequential architecture of tide-influenced alluvial deposits: An example from the middle Eocene Capella Formation, south-central Pyrenees, Spain: *Geologica Ultraiectina*, v. 61, p. 1–153.
- Harland, W.B., Armstrong, R.L., Cox, A.V., Craig, L.E., Smith, A.G., and Smith, D.G., 1990, *A geological time scale*: Cambridge, England, Cambridge University Press, 263 p.
- Hillhouse, J.W., Ndombi, J.W.M., Cox, A., and Brock, A., 1977, Additional results on paleomagnetic stratigraphy of the Koobi Fora Formation, east of Lake Turkana (Lake Rudolf), Kenya: *Nature*, v. 265, p. 411–415.
- Jackson, M.P.A., and Talbot, C.J., 1986, External shapes, strain rates, and dynamics of salt structures: *Geological Society of America Bulletin*, v. 97, p. 305–323.
- Kirschvink, J.L., 1980, The least-square line and plane and the analysis of paleomagnetic data: *Royal Astronomical Society Geophysical Journal*, v. 62, p. 699–718.
- Labatut, P., Séguret, M., and Seyve, C., 1985, Evolution of a turbiditic foreland basin and analogy with an accretionary prism: Example of the Eocene south-Pyrenean basin: *Tectonics*, v. 4, p. 661–685.
- Marzo, M., Nijman, W., and Puigdefábregas, 1988, Architecture of the Castisent fluvial sheet sandstone, Eocene, South Pyrenees, Spain: *Sedimentology*, v. 35, p. 719–738.
- Mutti, E., Séguret, M., and Sgavetti, M., 1989, Sedimentation and deformation in the Tertiary sequences of the southern Pyrenees: *American Association of Petroleum Geologists Mediterranean Basins Conference Guidebook*, Fieldtrip no. 7, Nice, France, University of Parma, Institute of Geology, Special Publication, 157 p.
- Nijman, W., and Nio, S.D., 1975, The Eocene Montanana delta, in Rossell, J., and Puigdefábregas, C., eds., *The sedimentary evolution of the Paleogene South Pyrenean basin*: Nice, France, International Association of Sedimentologists International Congress, p. 1–20.
- Ori, G.G., and Friend, P.F., 1984, Sedimentary basins formed and carried piggyback on active thrust sheets: *Geology*, v. 12, p. 475–478.
- Puigdefábregas, C., 1974, Les sédiments de marée du Bassin Eocène Sudpyrénéen: *Bulletin de la Centre Recherches Pau-SNPA*, v. 8, p. 305–325.
- Riba, O., 1976, Tectogenèse et sédimentation: Deux modèles de discordances syntectoniques pyrénéennes: [France] Bureau de Recherches Géologiques et Minières, Bulletin, sec. 1, p. 383–401.
- Roest, W.R., and Srivastava, S.P., 1991, Kinematics of the plate boundaries between Eurasia, Iberia, and Africa in the North Atlantic from Late Cretaceous to the present: *Geology*, v. 19, p. 613–616.
- Slater, J.G., and Christie, P.A.F., 1980, Continental stretching: An explanation of the post-mid-Cretaceous subsidence of the central North Sea basin: *Journal of Geophysical Research*, v. 85, p. 3711–3739.
- Séguret, M., 1972, Etude tectonique des nappes et séries décollées de la partie centrale du versant sud des Pyrénées [thesis]: Montpellier, Publications USTECA, 160 p.
- Stein, R.S., 1983, Reverse slip on a buried fault during the 2 May 1983 Coalinga earthquake: Evidence from geodetic elevation change, in Bennet, J.H., and Sherburne, R.W., eds., *The 1983 Coalinga, California, earthquake*: California Division of Mines and Geology Special Publication 66, p. 151–163.
- Zijderveld, J.D.A., 1967, A.C. demagnetization of rocks: Analysis of results, in Collinson, D.W., et al., eds., *Methods in paleomagnetism*: Volume 3, p. 254–286.

Manuscript received June 15, 1992
Revised manuscript received October 26, 1992
Manuscript accepted November 10, 1992